Chalcogenide Letters Vol. 14, No. 5, May 2017, p. 187 - 193

OPTIMIZATION OF POWER FACTOR IN SNDOPED $Tl_{10-x}Sn_xTe_6$ THERMOELECTRIC CHALCOGENIDENANO-MATERIALS

W. H. SHAH*, W. M. KHAN, S. TAJUDIN, M. TUFAIL, W. A. SYED
Department of Physics, Faculty of Basic and Applied Sciences, International Islamic University,
H-10, Islamabad, Pakistan

The electrical and thermal properties of the doped Tellurium Telluride ($Tl_{10}Te_6$) chalcogenide nano-particles are mainly characterized by a competition between metallic (hole doped concentration) and semi-conducting state. We have studied the effects of Sn doping on the electrical and thermoelectric properties of $Tl_{10-x}Sn_xTe_6$ ($1.00 \leq x \leq 2.00$), nano-particles, prepared by solid state reactions in sealed silica tubes and ball milling method. Structurally, all these compounds were found to be phase pure as confirmed by the x-rays diffractometery (XRD) and energy dispersive X-ray spectroscopy (EDS) analysis. Additionally crystal structure data were used to model the data and support the findings. The particles size was calculated from the XRD data by Scherrer's formula. The EDS was used for an elemental analysis of the sample and declares the percentage of elements present in the system. The thermo-power or Seebeck co-efficient (*S*) was measured for all these compounds which show that *S* increases with increasing temperature from 295 to 550 K. The Seebeck coefficient is positive for the whole temperature range, showing p-type semiconductor characteristics. The electrical conductivity was investigated by four probe resistivity techniques revealed that the electrical conductivity decreases with increasing temperature, and also simultaneously with increasing Sn concentration. While for Seebeck coefficient the trend is opposite which is increases with increasing temperature. These increasing behavior of Seebeck coefficient leads to high power factor which are increases with increasing temperature and Sn concentration except For $Tl_8Sn_2Te_6$ because of lowest electrical conductivity but its power factor increases well with increasing temperature.

(Received February 10, 2017; Accepted May 15, 2017)

Keywords: Sn doping in Tellurium Telluride nano-materials, Electron holes competition, Seebeck co-efficient, effects of Sn doping on electrical conductivity, Effects on Power factor,

1. Introduction

The increasing awareness of declining global energy resources alternative method of power generation for example the thermoelectric energy conversion becomes increasingly important.[1] Thermoelectric (TE's) materials with a wide working temperature range for different applications in cooling and power generation have been extensively studied [1-5]. Tellurium telluride (Tl_5Te_3) is one of the most studied and used intermediate temperature TE materials with good thermoelectric properties, suitable for power generation applications.

The effectiveness of thermoelectric generator is determined by the investigation of power factor, which is measured by the square of Seebeck coefficient multiplied by electrical conductivity at particular temperature, i.e. $PF=S^2\sigma$.The power factor depends substantially on details of the electronic band structure and carrier scattering mechanism. The important condition for achieving a large power factor is by maximizing the Seebeck co-efficient S^2 and minimizing electrical conductivity σ. These conditions can be achieved in materials, having complex band structure, high degree of degeneracy with several co-existing bonding types and scattering

*Corresponding author: wiqarhussain@yahoo.com

mechanism. A group of materials which satisfy these requirements are the Sn doped ternary compounds of $Tl_{10-x}Sn_xTe_6$. There is very limited information on the thermoelectric properties of Sn doped $Tl_{10-x}Sn_xTe_6$ nano-materials. Structural, electrical and thermoelectric properties of these compounds have been studied over temperature range 300 to 550 K as a function of deviation from stoichiometry.

To find the best material for efficient thermoelectric generator, we must choose the materials, which have high Seebeck effect, high electrical conductivity and low thermal conductivity. The only material with good electrical and thermal conductivity is metal because their band gap is overlapped (continues energy states), but their high thermal conductivity decreases the Seebeck co-efficient of the metals make it unsuitable for thermoelectric application, insulators which has a wide band gap due to which its electrical and thermal conductivity are low but not suitable for thermoelectric application because of low electrical conductivity.

The main objective of this work is to study and optimize the temperature dependence of the thermoelectric properties of Sn doped Tellurium Telluride $Tl_{10-x}Sn_xTe_6$ over a wide temperature range (295-550 K) and to evaluate the potential of these materials for the thermoelectric applications. To develop high-performance nano-materials for thermoelectric generator, we have investigated charge carriers injected (Sn doped) thallium compounds as these types of nano-materials have extremely low thermal conductivity as well as moderate electrical performance as compared to their bulk counterpart [6]. We have investigated the properties of $Tl_{10-x}Sn_xTe_6$ compound due to their low thermal conductivity and high electrical conductivity and potential for their use as high performance bulk thermoelectric materials.To optimize the properties, these materials are typically doped to get charge carrier concentrations of the order of 10^{19}-10^{21} carriers per cubic centimeter [7-9]. Heavy elements are known to contribute to low thermal conductivity an important asset of enhanced thermoelectric properties.

K. Kurosaki *et al*. [6] prepared the thallium antimony telluride $TlSbTe_2$ and investigated that the electrical resistivity is high and the thermal conductivity is low as compared to Sintered Bi_2Te_3 and TAGS "$(GeTe)_{1-x}(AgSbTe_2)_x$" material. The Seebeck coefficient of $TlSbTe_2$ is 224 μVk^{-1} at 666 K which is positive in the whole temperature range showing p-type behavior. The power factor ($S^2\sigma$) found for $TlSbTe_2$ is $8.9 \times 10^{-4}\ Wm^{-1}k^{-2}$ at 576 K which is low as compared the power factor of current thermoelectric devices i.e. in the range $10^{-3}\ Wm^{-1}k^{-2}$. Joseph P. Heremans *et al*. [4] uses the concept of electronic density of states to increase the power factor in lead telluride PbTe, the Seebeck coefficient was enhanced by deforming the electronic density of states, leads to double the power factor and further explained that in nanostructured material it may give us further improved results.

We have explored materials with more complex compositions and structures which is likely to have more complex electronic structures that could give rise to high TE performance. Good TE materials require an unusual combination of electrical and thermal properties, i.e. the challenge lies in achieving simultaneously high electrical conductivity σ, high TE power *S*, and low thermal conductivity k. All three of these properties are determined by the details of the electronic structure (band gap, band shape, and band degeneracy near the Fermi level, electronic concentrations) and scattering of charge carriers (electrons or holes) and thus are not independent from each other.

2. Experimental

The Sn doped $Tl_{10-x}Sn_xTe_6$ is (x=1.00, 1.25, 1.50, 1.75, 2.00) has been prepared by solid state reactions in evacuated sealed silica tubes. The purpose of this study were mainly for discovering new type of ternary and quaternary compounds by using Tl^{+1}, $Sn^{+3}$and Te^{-2} elements as the starting materials. Direct synthesis of stoichiometric amount of high purity elements i.e. 99.99 % of different compositions have been prepared for a preliminary investigation. Since most of these starting materials for solid state reactions are sensitive to oxygen and moistures, they were weighing stoichiometric reactants and transferring to the silica tubes in the glove box which is filled with Argon. Then, all constituents were sealed in a quartz tube. Before putting these samples in the resistance furnace for the heating, the silica tubes was put in vacuum line to evacuate the

argon and then sealed it. This sealed power were heated up to 650 C^o at a rate not exceeding 1 k/mint and kept at that temperature for 24 hours. The sample was cooled down with extremely slow rate to avoid quenching, dislocations, and crystals deformation.

Structural analysis of all these samples was carried out by x-rays diffraction, using an In el powder diffractometer with position-sensitive detector and CuKα radiation at room temperature. No additional peaks were detected in any of the sample discussed here. X-ray powder diffraction patterns confirm the single phase composition of the compounds.

The temperature dependence of Seebeck co-efficient was measured for all these compounds on a cold pressed pellet in rectangular shape, of approximately 5x1x1 mm^3 dimensions. The air sensitivity of these samples was checked (for one sample) by measuring the thermoelectric power and confirmed that these samples are not sensitive to air. This sample exposes to air more than a week, but no appreciable changes observed in the Seebeck values. The pellet for these measurements was annealed at 400 C^0 for 6 hours.

For the electrical transport measurements 4-probe resistivity technique was used and the pellets were cut into rectangular shape with approximate dimension of 5x1x1 mm^3.

3. Results and discussions

3.1. Structural analysis

X-ray diffraction is the most important technique for the determination of crystal structure of different materials, and for the determination of particle size. In order to check the purity of the compound, peaks in XRD data are matched with the literature [10], as shown in Fig. 1. It is substantiated that the XRD pattern of all these samples are well uniform with the literature and has been identified that the crystal structure system is isostructural with reference data of Tl_9GdTe_6 and Tl_9BiTe_6 having tetragonal crystal structure with the space group symbol of i4mcm and a substitutional variant of $Tl_{10}Te_6$ (Tl_5Te_3) [10, 18]. The crystal structure found for $Tl_{10-x}Sn_xTe_6$ is very complex with a unit cell volume changes between $V = 1005.505$ for $Tl_9Sn_1Te_6$ and $V = 1022.7177$ for $Tl_8Sn_2Te_6$.

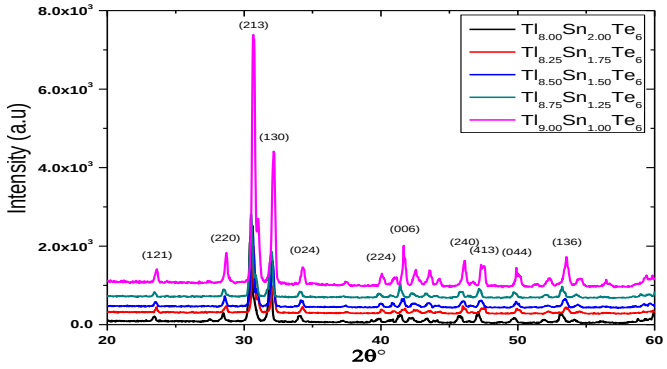

Fig. 1: XRD data of $Tl_{10-x}Sn_xTe_6$ with $Sn = 1, 1.25, 1.50, 1.75$ and 2, collected at room temperature

The XRD patterns of $Tl_{10-x}Sn_xTe_6$(x=1.00, 1.25, 1.50, 1.75, 2.00) as shown in Fig.1 has been clearly observed that the unit cell volume increases with increase in Sn contents as shown in table 1.

Table1. Crystallite size, Lattice constant and Volume of unit cell.

Sample	Crystallite size, $D = 0.9\lambda/\beta\cos\theta$ (nm)	Lattice constant $a, b, c =$ (Å)	Volume (Å^3)
$Tl_9Sn_1Te_6$	62.919	a = b = 8.7930 c = 13.0050	1005.505
$Tl_{8.75}Sn_{1.25}Te_6$	63.965	a = b = 8.8450 c = 13.0755	1022.948
$Tl_{8.50}Sn_{1.50}Te_6$	66.2833	a = b = 8.8250 c = 13.0000	1012.44
$Tl_{8.25}Sn_{1.75}Te_6$	59.820	a = b = 8.8100 c = 13.0010	1009.086
$Tl_8Sn_2Te_6$	56.793	a = b = 8.8484 c = 13.0625	1022.717

3.2. Energy Dispersive X-ray Analysis

The Energy Dispersive X-ray Analysis (EDX) has been used to investigate the qualitative analysis of the various samples. Fig. 4.2 (a) and (b) represent EDX spectrums of *Sn* nanoparticles doped in $Tl_{10}Te_6$ with Sn=1, 1.25, 1.50, 1.75 and 2. From the spectrum it has indicated that the sample is consist of 6.99% Sn, 27.26% Te and 65.75% Tl content in $Tl_8Sn_2Te_6$ (Fig. 4.2) and 7.12% *Sn*, 27.25% Te and 65.63% Tl concentration in $Tl_9Sn_1Te_6$ Shown in Fig. 2.

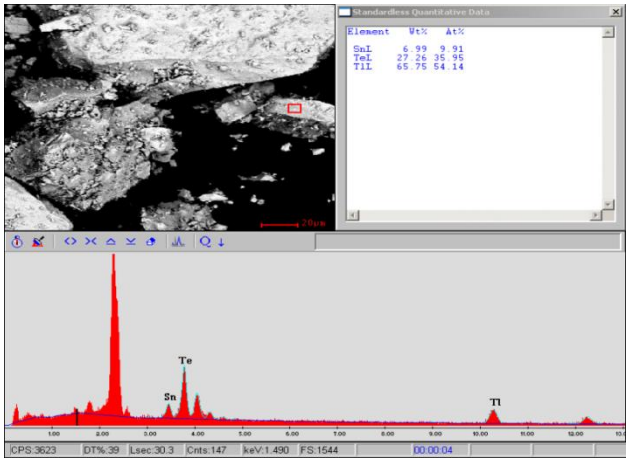

Fig. 2. EDX data for $Tl_{10-x}Sn_xTe_6$ (x= 1.0, 1.25, 1.50, 1.75, 2.00, collected at room temperature are shown here, to conform the elemental analysis in the system, with all other compounds have the same stoichiometric ratio as designed

3.3. Physical properties

To investigate the impact of reduction of the charge carriers in thermal and transport characteristics Sn content was increased in $Tl_{10-x}Sn_xTe_6$ (x=1.00, 1.25, 1.50, 1.75, 2.00) by replacing Tl atoms according to the formula. The temperature variation as a function of the Seebeck co-efficient (S) for the $Tl_{10-x}Sn_xTe_6$ (x=1.00, 1.25, 1.50, 1.75, 2.00) compounds are shown in Fig. 3.The Seebeck coefficient was measured in the temperature gradient of 1 K. The positive Seebeck co-efficient increases smoothly with increasing temperature from 300 K to 550 K, for all compounds in particularly for p-type semiconductors having high charge carrier concentration. It is obvious that all the samples exhibit positive Seebeck coefficient for the entire temperature range, indicating that the p-type (hole) carriers conduction dominates the thermoelectric transport in these compounds. When the amount of Sn increased from 1.00 to 2.00, the Sn doping is supposed to increase the carrier's density. However, the smaller grains upon Sn doping are believed to be able to enhance the electron scattering, yielding an increase of the Seebeck co-efficient and effective mass [10-14]. It was found that only an appropriate amount of Sn doping

could improve the Seebeck co-efficient in this particular system. In other words the Seebeck co-efficient will drop drastically on doping from the optimum value of Sn concentration. Further improvements could be achieved by (i) employing a rapid fabrication procedure such as melting spinning to reduce the grain size to a much greater degree, (ii) optimizing the doping elements and their corresponding amounts to simultaneously improve the charge mobility and carrier density in order to concurrently enhance the Seebeck co-efficient [13].

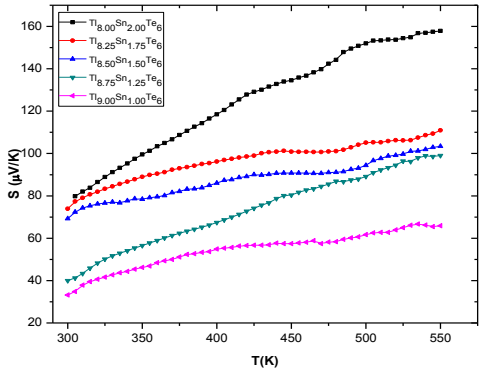

Fig. 3. Temperature dependence of Seebeck Co-efficient of of $Tl_{10-x}Sn_xTe_6$ (x= 1.0, 1.25, 1.50, 1.75, 2.00)

The temperature variations of electrical conductivity of the quaternary compounds are shown in Fig. 4. The conductivity observed for all the samples studied here, decreases with increasing temperature, indicating the degenerate semiconductor behavior due to positive temperature co-efficient, resulting from the phonons scattering of charge carriers and grains boundaries effects [15].An increasing *x* value, (i.e. increasing the Sn deficiency) is expected to increase the number of holes, which is experimental observed. The smaller temperature dependence may be caused by (less temperature dependence) more grain boundary scattering. No systematic trend was found in the variation of the electrical resistivity for samples $Tl_{10-x}Sn_xTe_6$ (x=1.00, 1.25, 1.50, 1.75, 2.00) with Sn concentration. The low electrical conductivity in the pressure less sintered sample [15-19] may be caused by the oxide impurity phase in the grain boundary and the number of the grain boundary. The *Pb* doping level and grain boundary resistance may play important role for increasing electrical conductivity.

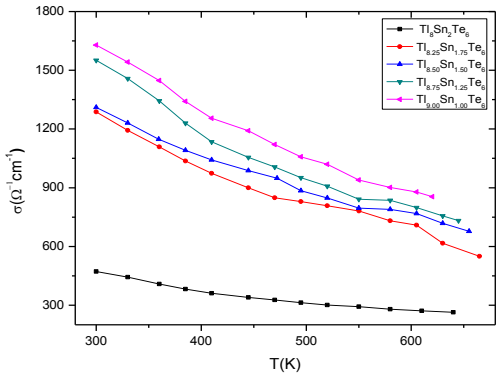

Fig. 4. Temperature dependence of electrical conductivity of $Tl_{10-x}Sn_xTe_6$ (x= 1.0, 1.25, 1.50, 1.75, 2.00) of the cooled pressed pellet, with heating profile

The band structure calculations for $Tl_9Sb_1Te_6$ and $Tl_8Sn_2Te_6$ suggest that $Tl_8Sn_2Te_6$ is a heavily doped p-type semiconductor with a partially empty valence band, while the Fermi-level in $Tl_8Sn_2Te_6$ is located in the band gap [5]. In accord with these calculations, both thermal and

electrical conductivity measurements indicate that increasing Sn contents results in lower values, as determined on sintered polycrystalline samples. For the Seebeck co-efficient, we have observed an opposite trend increasing Sn concentration, causes Seebeck values increases.

The electrical conductivity σ for the $Tl_{10-x}Sn_xTe_6$ compounds with $1.00 \leq x \leq 2.00$ as shown in Fig.4 decreases with increase in temperature across the entire temperature range examined. These results are the indicative of metallic behavior, an evidence of a relatively high carrier concentration. Increased, doping concentration causes decrease in σ as expected and inversely affecting their Seebeck counterpart [20]. The sample with x=1.00 i.e. $Tl_9Sb_1Te_6$ displays the highest value of electrical conductivity i.e. 1711 $(\Omega\text{-cm})^{-1}$ at 295 K, and$Tl_8Sb_2Te_6$ reveals the lowest with 445$(\Omega\text{-cm})^{-1}$and the samples with x= 1.25 and 1.50 almost have very close values of about 1315 and 1325$(\Omega\text{-cm})^{-1}$ respectively. The conductivity differences at room temperature between the hot pressed pellet and the ingot was observed a little change from 1315 to 1355$(\Omega\text{-cm})^{-1}$respectively for the $Tl_{8.5}Sb_{1.5}Te_6$ compound.

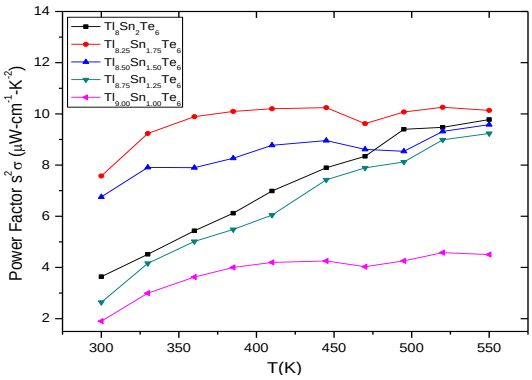

Fig. 5 Variation of Power factor with temperature and their dependency on doping concentration for $Tl_{10-x}Sn_xTe_6$ (x= 1.0, 1.25, 1.50, 1.75, 2.00)

To enhance the power factor (PF=$S^2\sigma$) for these compounds, we need to decouple the electrical conductivity from the Seebeck co-efficient, usually inversely proportional to each other in these systems. The main contribution in the PF comes from the Seebeck co-efficient, so we have to design the materials such that their *S* should be enhanced. The power factors calculated from the electrical conductivity σ and the Seebeck co-efficient S obtained for $Tl_{10-x}Sn_xTe_6$ compounds with $1.00 \leq x \leq 2.00$ are displayed in Fig. 5. The power factor increases with increasing temperature for all these compounds. The doping concentration shows a systematic effect on the power factor as increasing the doping concentration, the power factor is increases. The $Tl_8Sb_2Te_6$ compound displayed the highest value 9.56 (μWtt-cm^{-1}-K^{-2}) of PF at 550 K and 7.25 (μWtt-cm^{-1}-K^{-2}) at 290 K. The lowest PF factors were observed for $Tl_9Sb_1Te_6$ compound which have values of 4.13 (μWtt-cm^{-1}-K^{-2}) at 550 K and 1.75(μWtt-cm^{-1}-K^{-2}) at 290 K. As discussed before, an increasing the Sn deficiency is expected to increase the number of holes, the dominant charge carriers. This expected trend is experimental observed with increasing x, the Seebeck co-efficient increases with *Sn* concentration, which results in increase in the S. The smaller temperature dependence for some compounds may be caused by (less temperature dependence) more grain boundary scattering.

4. Conclusions

In order to interpret our results, we start by concluding the basic understanding of the metallic long-range interactions, and semiconducting frustration effects leading to metallic like behavior in these chalcogenide nano-system. The structural investigation revealed that $Tl_{10-x}Sn_xTe6$ single phase, all peaks are corresponding to their respective element and no extra peaks are observed, which conferring expected crystal structure for our design materials and also shows that there are no impurities or dislocation in the sample. EDS study confirms the percentage of

elements present in the sample. The electrical characterizations shows that parent compounds behaves like a semiconductor, but increasing the *Sn* contents, this nano-materials tend toward the metallic properties, which show that increasing the temperature the electrical conductivity will decreases at higher temperature.

The thermopower is positive in the entire temperature studied here, which is increasing with increase in temperature, indicating that the nano-particles under investigation is hole conduction dominated. For higher concentrations of *Sn*, the Seebeck co-efficient of the doped tellurium telluride is decreasing due to increasing hole concentration which in turns increasing the electron scattering in this doped chalcogenide system. However, the smaller grains upon Sn concentrations will enhance the electron scattering, resulting increase in thermopower. Consequently, power factor was enhanced and increased with high Sn concentration up to $\mathrm{Sn} = 1.75$ and the maximum power factor ($PF = 7.58\ \mu W cm^{-2} K^{-2}$) was observed for $Tl_{8.25}Sn_{1.75}Te_6$. This improved power factor will enhance the thermoelectric efficiency and results good thermoelectric applications, which is the main goal of this work. At the end, we are going to conclude that this work is the best example of optimizing dopants concentration to achieve desirable thermoelectric properties in *Sn* doped $Tl_{10-x}Sn_xTe_6$ chalcogenide system.

References

[1] T. Caillat, J. Fleurial, A. Borshchevsky, AIP conf. Proc. **420**, 1647 (1998).
[2] R. J. Campana, Adv. Ener. Conv. **2**, 303 (1962).
[3] R.J. Mehta, Y Zhang, C. Karthika eta, Nature Materials, **11**, 233-240 (2012).
[4] G.S. Nolas, J. Poon and M. Kanatzidis, MRS, Bull **31**199 (2006),
[5] B.A. Kuropaatawa, A. Assoud, H. Klienke, J. Alloys and Compounds **509**, 6768 (2011).
[6] K. Kurosaki, A. Kosuge, H. Muta, M. Uno, and S. Yamanaka, Applied Phys. Letts. **87**, 061919 (2005); J. Yang, F.R. Stablers, J. Electrn.Mater.**38**, 1245 (2009).
[7] G.J. Synder, E.S. Toberer, Nat. Mater. **7**, 105 (2008).
[8] J.R. Soostsman, D.Y. Chung, Kanatzdis, M.G. Angew Chem. Inter. Ed. **48**, 8616 (2009).
[9] E.S. Toberer, A.F. May, G.J. Synder Chem. Mater. **22**, 624 (2010).
[10] Y. K. Kurosaki, "Thermoelectric properties of Tl9BiTe6," *Journal of Alloys and Compounds*, p. 275, 2003, A. Pradel, J.C Tedenac, D. Coquillat, G. Burn, Rev. Chim. Miner. **19**, 43 (1982)
[11] S.Y. Wang, G.J. Tan, W.j. Xie, G. Zheng, H. Li, J.H. Yang, and X.F. Tang, J. Mater. Chem. **22**, 20943 (2012)
[12] H. Wang, A.D. Lalonde, Y. Pie, and G.J Synder, Adv. Funct. Mater.**23**, 1586 (2013).
[13] Z. Cai, L. Guo, X. Xu, Y. Yan, K. Peng, G. Wang, and X Zhou, J. Electronic Mater. **45**, 1441 (2016).
[14] K.T. Kim, T.S. Lim, G.H. Ha, Rev. on Advanced Materials Science **28**, 196 (2011)
[15] H. Unuma, N. Shigetsuka, M. Takahashi, J. Mater. Sci. Lett. **17**, 1055 (1998).
[16] H.J. Goldsmid, J.W. Sharp, J. Electron. Mater.**28**, 869-872, (1999)
[17] K.F. Hsu, S. Loo, F. Guo, W Chen, J.S. Dyck, C. Uher, T. Hogan, E.K. Polychroniadis, M.g. Kanatzidis, Nature **489**, 414 (2012)
[18] Y. K. Kurosaki, "Thermoelectric properties of Tl9BiTe6," *Journal of Alloys and Compounds*, p. 275–278, 2003.
[19] S. Bangarigadu-Sansay, C.R. Sankar, P. Schlender, H. Klienke, J. Alloys and compounds **594**, 126 (2013).
[20] Wiqar H Shah, Aqeel Khan, Waqas Khan, Waqar Adil Syed, Chalcogenide Letters, **14**, 61 (2017)